The 2010 IEEE/RSJ International Conference on
Intelligent Robots and Systems
October 18-22, 2010, Taipei, Taiwan

# A 3-Way Valve-Controlled Spring Assisted Rotary Actuator

Yousheng Yang, Emanuele Guglielmino, Claudio Semini, Jian S. Dai and Darwin G. Caldwell

*Abstract*— **Hydraulic actuators are characterized by fast dynamics, high power density, high stiffness, large output force/torque, and in recent years are becoming increasingly attractive in the field of robotics. This paper presents the study of a 3-way proportional valve controlled, spring assisted electro-hydraulic rotary actuator, which consists of a 3-way proportional valve, a linear cylinder and a reciprocal spring. The operating principle is presented and a mathematical model is developed. Comparison analysis is made between the new actuator and a traditional one with an application to a hydraulically actuated legged robot.**

## I. Introduction

Hydraulic actuation is a classical actuation technique, however, recently this form of actuation has not been considered in robotics. This lack of acceptance is mainly due to the nature of the hydraulic systems and the ease of use of the electric systems. Hydraulic actuation is often believed to be dirty, noisy, complicated to use. It has low efficiency, and is hard to package; friction and complex dynamics makes its control difficult. This is certainly true. However, many of these shortcomings have been or are going to be overcome through recent the development in technology.

A recent development is the use of water instead of oil as pressure transmitting medium [1, 2]. Water is an interesting alternative to oil since it is environmentally friendly, non-flammable, inexpensive, clean, readily available, and easily disposable. Most important, it can achieve higher dynamic performance as is stiffer than oil.

One of the key components of these robots is the electro-hydraulic actuator. Hydraulic actuators specifically designed for robotics and other demanding applications, overcome many of the above-mentioned shortcomings and offer a unique set of performance characteristics.

In terms of efficiency, an effective way to reduce energy loss in hydraulic components is the use of protective hard coatings [3, 4]. They are applied to the contacting surfaces, which reduces the friction, wear and material degradation. Other solutions involve the use of on-off valve instead of proportional valves [5].

Although some shortcomings of hydraulic actuation are not yet solved, it offers advantages such as high power density, overload protection, reliability and ruggedness. A key advantage is that they can deliver a great deal of power relative to their inertia. Other attractive features are the high stiffness of hydraulic fluids which leads to a high natural frequency. Therefore in very recent years there have been a number of high profile robotic systems that have used hydraulic actuation. Among the best known examples are: the exoskeleton system BLEEX [6] and Raytheon SARCOS [7], the SARCOS hydraulically actuated humanoid robot CB [8], the legged robots like Kenken [9], BigDog [10], Petman [11] and the prototype HyQ [12-15].

Our research aims at the development of a high performance actuator for hydraulically actuated legged robots. This paper focuses on the modeling of a 3-way proportional valve controlled, spring assisted electro-hydraulic rotary actuator. The operating principle is presented and a physical model is derived. Investigations are performed on the output torque and the volumetric displacement.

The paper is organized as follows: Section II states the problems of conventional hydraulic actuators. Section III introduces the configuration and function of the new design. Section IV presents the mathematical model, and Section V focuses on the comparison of the two solutions. Finally, section VI addresses the conclusions.

## II. Statement of Problem

Usually, symmetric 4-way proportional valve controlled asymmetric cylinders are used in hydraulically actuated robots [6-15] (Fig.1). This section discusses some of the problems associated with this classical type of actuation and presents possible solutions.

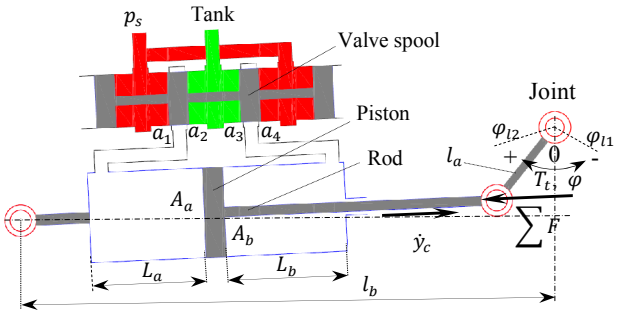


Fig.1 Joint actuated by 4-way valve controlled cylinder

### A. Pressure jumps

Due to the interaction between the valve and cylinder, high pressure jumps occur in the actuator chamber when reversing the direction of motion. The system governing equations can be written as:

$$p_a A_a - p_b A_b = \sum F = F_t + F_f + C_r \dot{y}_c + M_c \ddot{y}_c \tag{1}$$

$$\dot{y}_c = \frac{a_1}{A_a} C_q \sqrt{\frac{2}{\rho}(p_s - p_a)} - \frac{a_2}{A_a} C_q \sqrt{\frac{2}{\rho} p_a} - \frac{L_a}{\beta_e} \dot{p}_a \tag{2}$$

Y. S. Yang, E. Guglielmino, C. Semini, J. S. Dai and D. G. Caldwell are with the Italian Institute of Technology, Via Morego 30, 16163 Genoa, Italy. hptc_yang@163.com; {emanuele.guglielmino; claudio.semini; jian.dai; darwin.caldwell}@iit.it.

$$\dot{y}_c = \frac{a_3}{A_b} C_q \sqrt{\frac{2}{\rho} p_b} - \frac{a_4}{A_b} C_q \sqrt{\frac{2}{\rho}(p_s - p_b)} + \frac{L_b}{\beta_e} \dot{p}_b \tag{3}$$

where $p_s$ is the supply pressure, $p_a$ and $p_b$ are the pressures in the two cylinder chambers, $A_a$ and $A_b$ are the piston areas, $y_c$ is the cylinder displacement, $\sum F$ is the total load, $F_t$ is the load acting on the cylinder rod, $F_f$ the friction force, $C_r$ the damping coefficient, $M_c$ the mass, $C_q$ the flow coefficient, $\rho$ the fluid density, $\beta_e$ the bulk modulus and $a_i$ $(i = 1{\sim}4)$ the flow area of the valve.

From (1)-(3), the pressures in the two actuator chambers can be obtained. They are listed in Table I under the assumptions that the fluid is incompressible, the actuator and valve have good sealing and the valve is symmetric.

TABLE I
PRESSURES IN ACTUATOR CHAMBERS

| | $p_a$ | $p_b$ |
|---|---|---|
| $\dot{y}_c > 0$<br>$a_1 = a_3 > 0$<br>$a_2 = a_4 = 0$ | $\left(p_s + \frac{\sum F}{A_a} r^3\right) \frac{1}{1+r^3}$ | $\left(p_s - \frac{\sum F}{A_a}\right) \frac{r}{1+r^3}$ |
| $\dot{y}_c < 0$<br>$a_2 = a_4 > 0$<br>$a_1 = a_3 = 0$ | $\left(p_s - \frac{\sum F}{A_b}\right) \frac{r^2}{1+r^3}$ | $\left(r^3 p_s + \frac{\sum F}{A_b}\right) \frac{1}{1+r^3}$ |

where $r = A_a/A_b$ .

From Table I, it can be seen that both the piston area ratio $r$ and the total load acting on the actuator have a significant effect on the pressure jumps. Even if $\sum F = 0$, there still exist pressure jumps in the actuator chambers when reversing, in other words, it is not possible for the actuator to work smoothly near $\dot{y}_c = 0$.

### B. Risk of buckling

Another disadvantage is a high risk of buckling. Using a linear cylinder to realize a rotary movement, the actuator has two motions, (Fig.2): linear reciprocating and rotary motions [14] and can be expressed as:

$$\begin{aligned} \dot{\varphi}_c &= \frac{d\varphi_c}{d\varphi}\dot{\varphi}, \varphi_c = \operatorname{actan}\frac{l_a(1-\cos\varphi)}{l_b - l_a \sin\varphi} \\ \dot{y}_c &= \frac{dl_c}{d\varphi}\dot{\varphi}, l_c = \sqrt{l_b^2 + 2l_a^2 - 2l_a(l_b \sin\varphi + l_a \cos\varphi)} \end{aligned} \tag{4}$$

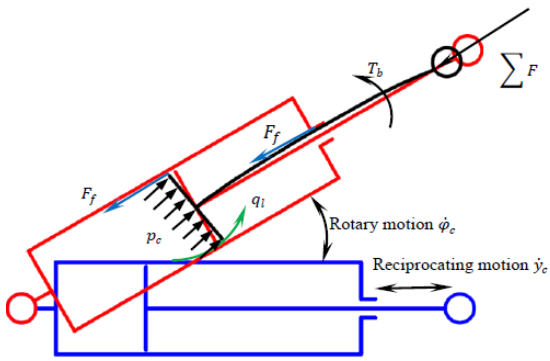


Fig.2 A cylinder in rotary motion: during this motion it experiences a linear (reciprocating) motion and a rotary motion

From (4), it can be seen that the rotary motion is nonlinear, which implies the presence of angular acceleration and torque $T_b$ acting on the actuator. Furthermore, when the actuator extends, a compressive force acts on the rod end. This causes the rod to bend (and under high loading even break) and the piston to incline, thus resulting in large leakage and great friction force.

### C. Energy losses

Hydraulic control valves are based on the orifice principle throttling the fluid flow and generating significant energy losses. For a 4-way valve controlled actuator, there are always two orifices working together. The energy loss $\Delta E$ of an orifice is defined as:

$$\Delta E = \int_{t_1}^{t_2} \Delta p q \, dt \tag{5}$$

where $\Delta p$ is the pressure drop and $q$ is the flow rate.

From (1) - (3), the total energy loss in a 4-way valve for one cycle is:

$$\begin{aligned} \Delta E = &\int_{nT}^{nT+t_c} A_a \dot{y}_c \left(p_s - \sum F/A_a\right) dt \\ &+ \int_{nT+t_c}^{(n+1)T} A_b \dot{y}_c (p_s - \sum F/A_b)\, dt \end{aligned} \tag{6}$$

From (6), it can be seen that the energy loss mainly depends on the difference between the system pressure and the total load pressure $\sum F/(A_a$ or $A_b)$and that the closer the total load pressure to the system pressure, the less the energy loss. However, for a position feedback control system, the system pressure $p_s$ is set by a relief valve. The total load applied to the actuator for a legged robot changes significantly [16], especially during jumping. Hence the maximum total load can be more than ten times the minimum total load; hence the energy loss will be very large in the 4 way valve-controlled actuators.

### D. Solutions

One solution to reduce the energy loss is to control the system pressure with a force control strategy. However, actuators are velocity sources, i.e. a given controlled flow rate into the actuator results in a certain velocity. Moreover, these actuators are typically designed for position control. They are therefore by construction, high impedance (mechanically stiff) system, which makes force control very sensitive to control parameters often leading to instability. Moreover, uncertainties due to friction and leakage and noise in the force measurement (if force is measured using pressure sensors), make force a difficult quantity to control [17].

Another solution is pump flow control [18], which requires an independent pump is needed for each actuator. The position is controlled by adjusting the speed or the displacement of the pump. Because there are no control valves between the pumps and actuators, nor bypass relief valve, the energy loss is small and the efficiency of pump-controlled hydraulic actuation systems is high.

However, for each DOF, an actuator, a pump, a motor/engine and a switch valve are required, resulting in a larger size and weight compared to a valve-controlled hydraulic actuation system. Furthermore, pump-controlled systems response is below the 20 to 30 Hz range [18], which is too low to be suitable for many applications that are controlled by servo and proportional valves.

The third solution, presented this paper, is to design a new electro-hydraulic actuator. The higher efficiency is achieved by reducing throttle orifices and less flow is required by making the actuators work alternately and using springs as power storage for a reciprocal motion (spring energy storage is useful in walking robot) [14].

## III. PHYSICAL MODEL

### A. Configuration

The configuration of the 3-way valve controlled spring assisted rotary actuator is illustrated in Fig.3 (a). It consists of a 3-way proportional valve, a single-acting cylinder, a rotary joint, timing belt and a retracting spring.

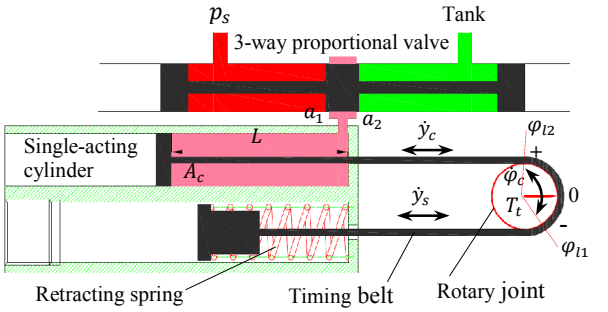


(a) Closed valve

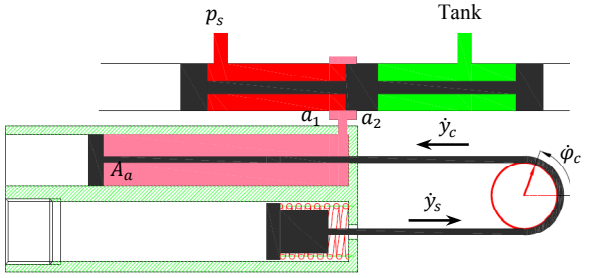


(b) Port $P_s$ to port $A$

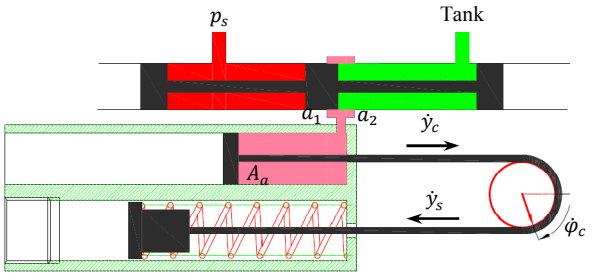


(c) Port $A$ to tank

Fig.3 3-way valve-controlled spring assisted rotary actuator in the three operating modes

### B. Function

As shown in Fig.3, instead of 4-way valves and double acting cylinders, a 3-way electro-hydraulic proportional valve is used to control a single acting cylinder that drives a joint by a timing belt. There exist three operation modes:

*a) Static mode*

$a_1 = a_2 = 0$, $\dot{y}_c = \dot{y}_s = 0$, $\varphi_c = \dot{\varphi}_c = 0$, the valve spool is at neutral position and the joint angle remains as they are. The pressure $p_{c0}$ in the cylinder chamber equals $p_s/2$ due to the leakage and the identical gaps from the $p_s$ port to the output port and from the output port to the tank. Under the action of pressure, the spring is compressed. If, in the static operation mode, we define the compression as $y_{s0}$ and the cylinder displacement as $y_{c0}$, this yields

$$p_{c0}A_c = p_sA_c/2 = k_sy_{s0} \tag{7}$$

*b) Active mode*

$a_1 > 0, a_2 = 0, \dot{y}_c > 0, \dot{y}_s < 0, \dot{\varphi}_c > 0$, the valve spool is at the right position and the cylinder chamber connect the power supply $p_s$, under the action of high pressure fluid, the cylinder retracts and compresses the spring. The joint turns anti-clockwise. In this operation mode high pressure flow is needed to drive the actuator.

*c) Passive mode*

$a_2 > 0, a_1 = 0, \dot{y}_c < 0, \dot{y}_s > 0, \varphi_c < 0$, the valve spool is at left position and the cylinder chamber connects to the tank. Under the action of the compressed spring, the cylinder extends. The fluid goes to tank through the controllable orifice $a_2$. The joint turns clockwise. In this operation mode, no flow is required to drive the actuator.

## IV. MATHEMATICAL MODEL

The assumptions made in the model include incompressible fluid, no friction and no sliding between the timing belt and joint ($\dot{y}_c = \dot{y}_s$), no flexibility in the timing belt, linear retracting spring, no leakage in the cylinder, symmetry of the valve land.

### A. 3-way proportional valve

The pressure-flow equations of an overlapped (i.e. the spool land is larger than the port resulting in a dead zone) spool valve can be written as:

$$q_c = C_q w f(x_s)[x_s - f(x_s)x_{s0}]\sqrt{\frac{p_s + f(x_s)(p_s - 2p_l)}{\rho}} \tag{8}$$

where $w$ is the area gradient, $f(x_s) = 0.5[sgn(x_s - x_{s0}) + sgnxs+xs0$, $xs$ the valve stroke, $xsm$ the maximum valve stroke and $x_{s0}$ the overlap length. A normalized plot of (8) is shown in Fig.4.

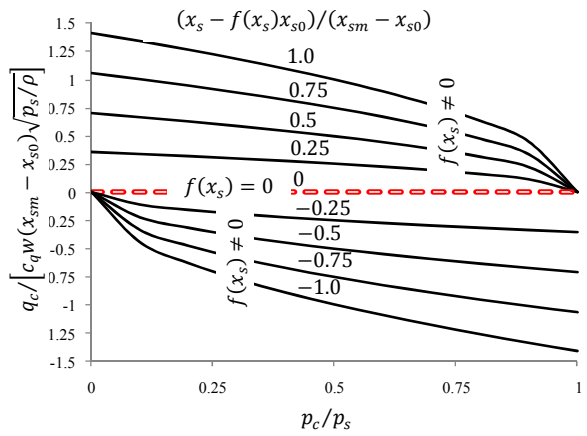


Fig.4 Pressure-flow relationship of overlap 3-way spool valve

From (8), the coefficients of the overlapped three-way spool valve are [18]:

The flow gain $k_q$

$$k_q \equiv \frac{\partial q_c}{\partial x_s} = C_q w f(x_s)\sqrt{[p_s + f(x_s)(p_s - 2p_l)]/\rho} \tag{9}$$

The flow pressure coefficient $k_c$

$$k_c \equiv -\frac{\partial q_c}{\partial p_l} = C_q w f(x_s)[x_s - f(x_s)x_{s0}]\frac{1}{\sqrt{\rho[p_s + f(x_s)(p_s - 2p_l)]}} \tag{10}$$

The pressure sensitivity coefficient $k_p$

$$k_p \equiv \frac{\partial p_l}{\partial x_s} = \frac{p_s + f(x_s)(p_s - 2p_l)}{x_s - f(x_s)x_{s0}} \tag{11}$$

The linearized equation of the pressure-flow curves of the 3-way valve can be written as:

$$dq_c = k_q dx_s - k_c dp_c \tag{12}$$

*B. Spring assisted rotary actuator*

*1) Cylinder*

According to Section III, the cylinder has two operation modes: active mode and passive mode (Fig. 5). By defining $y_c = 0$ when the actuator is at static mode, (Fig. 5(a)), the cylinder motion can be expressed as:

$$p_c A_c - F_c - C_f F_f = C_r \dot{y}_c + M_c \ddot{y}_c \tag{13}$$

$$y_c = r \cdot \varphi_c \tag{14}$$

where $p_c$ is the pressure in the cylinder chamber, $A_c$ is the rod area, $F_c$ is the cylinder output force, $F_f$ is the friction force, $C_f = sgn(\dot{y}_c)$, $C_r$ is the damping coefficient, $M_c$ is the mass of the piston and rod and $r$ is the joint radius.

*2) Spring-mass*

The spring is always compressed (Fig. 6). If we neglect the negligible spring damping and the friction force between the spring seat and the sleeve, the function of the spring-mass system can be written as:

$$-k_s(y_{s0} + y_s) + F_s = M_1 \ddot{y}_s + 0.5 M_s \ddot{y}_s \tag{15}$$

$$y_s = r \cdot \varphi \tag{16}$$

where $k_s$ is the spring constant, $y_{s0}$ the spring pre-compression, $y_s$ is the relative compression (defined in Fig.6), $F_s$ is the spring output force, $M_1$ is the mass of the spring seat, $M_s$ is the spring mass.

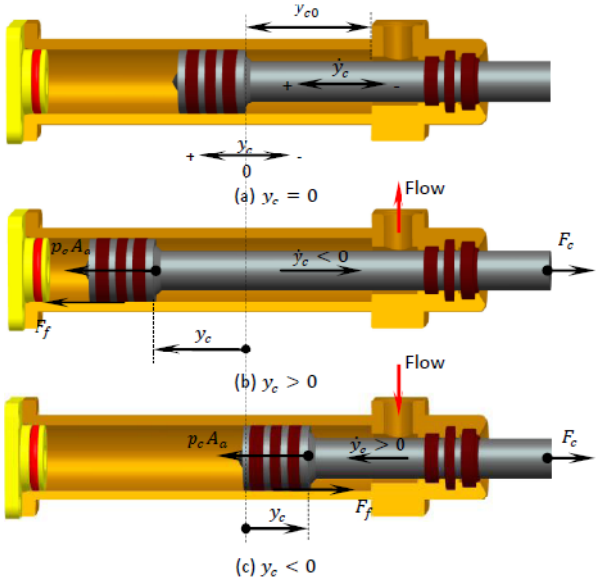


Fig.5 Motion and force definition of the cylinder: (a) static mode, the pre-displacement is $y_{c0}$ , the relative displacement is 0; (b) passive mode, the cylinder extends under the action of the compressed spring, $\dot{y}_c < 0$; (c) active mode, the cylinder retracts, $\dot{y}_c > 0$

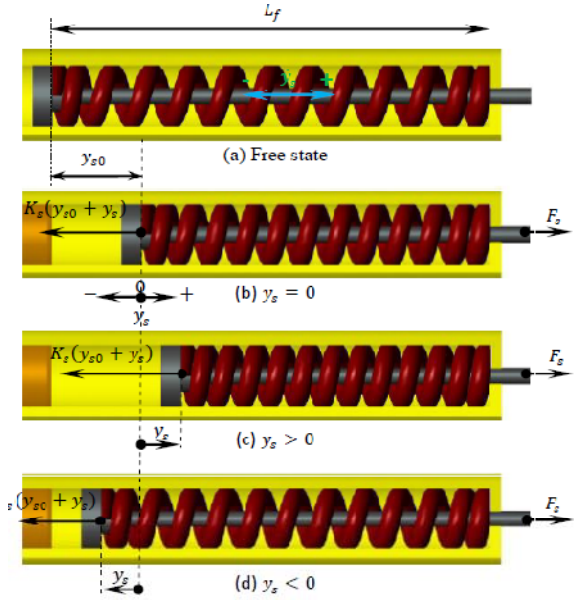


Fig.6 Motion and force definition of the spring: (a) free state; (b) static mode, the pre-compression is$y_{s0}$ , the relative compression is 0; (c) passive mode, continues spring compression under the action of the cylinder, $\dot{y}_s > 0$; (d) active mode, the spring extends, $\dot{y}_s < 0$.

*3) Rotary joint*

From Fig.3, the equation for the motion of the rotary actuator can be written as:

$$(F_c - F_s)r = T_t + G_s\varphi + D_r\dot{\varphi} + J\ddot{\varphi} \tag{17}$$

where $T_t$ is the total load torque, $G_s$ the torsional spring

stiffness, $D_r$ the load damping coefficient, $J$ the load rotary inertia. From (12)-(17) we obtain:

$$p_c A_c r - k_s y_{s0} r - C_f F_f r = T_t + G_{st}\varphi + D_{rt}\dot{\varphi} + J_t\ddot{\varphi} \quad (18)$$

where $G_{st} = G_s + k_s r^2$ is the total torsional spring stiffness, $D_{rt} = D_r + C_r r^2$ the total damping ratio and $J_t = (M_1 + M_c + 0.5M_s)r^2 + J$ the total rotary inertia.

Transformed by Laplace, (18) can be expressed as:

$$p_c A_c r - \frac{k_s y_{s0} r}{s} = \frac{C_f F_f r}{s} + T_t + G_{st}\varphi + D_{rt}\varphi s + J_t \varphi s^2 \quad (19)$$

Application of the continuity equation to the control volume in Fig. 3 (a) yields:

$$q_c - C_l p_c = A_c \dot{y}_c + \frac{V_0 + A_c y_c}{\beta_e}\dot{p}_c \quad (20)$$

If very small piston motions are assumed i.e. $|Ay_c| \ll V_0$, (21) can be transformed by Laplace:

$$q_c = C_l p_c + A_c y_c s + \frac{V_0}{\beta_e} p_c s \quad (21)$$

where $V_0$ is the initial rod chamber volume, $A$ is the rod side area, $\beta_e$ the fluid bulk modulus, $y_c$ cylinder displacement, $\varphi$ the joint angle and $C_l$ the cylinder leakage coefficient. According to (12) and (21), we obtain:

$$p_c = \frac{k_q x_s - A_c r \varphi s}{k_c + C_l + \frac{V_0}{\beta_e} s} \quad (22)$$

From (20) and (24), the transfer function of the output angle $\varphi$ can be written as:

$$\varphi = \frac{\frac{k_q}{A_c r} x_s - \frac{k_{cl}}{(A_c r)^2}\left(1 + \frac{V_0}{\beta_e k_{cl}} s\right)\left(T_t + \frac{r}{s}\left(k_s y_{s0} + C_f F_f\right)\right)}{B(s)}$$

$$B(s) = \frac{V_0 J_t}{\beta_e (A_c r)^2} s^3 + \frac{k_{cl}}{(A_c r)^2}\left(J_t + \frac{V_0 D_r}{\beta_e k_{cl}}\right) s^2 + \left(1 + \frac{k_{cl} D_r}{(A_c r)^2} + \frac{V_0 G_{st}}{\beta_e (A_c r)^2}\right) s + \frac{k_{cl} G_{st}}{(A_c r)^2} \quad (23)$$

where $k_{cl} = k_c + C_l$ total flow-pressure coefficient.

Equation (24) gives the actuator response to both valve position and load torque inputs. The system characteristic equation is third order and $J_t$, $D_{rt}$ and $G_{st}$ are lumped coefficients representing the total acceleration, velocity, position dependent torques, respectively.

## V. Comparison Study

A series of comparisons between the two types of actuators have been done with the same reference input. The evaluation of the performance was based on theoretical analysis.

### A. Specification

The parameters of the traditional actuator (used in [13-15]) and the new actuator are shown in Table II.

TABLE II
ACTUATOR SPECIFICATIONS

| Parameter | Value | |
|---|---|---|
| | Traditional | New |
| Cylinder stroke | 70 mm | 80 mm |
| Piston dia. | 16 mm | 20 mm |
| Rod dia. | 10 mm | 10 mm |
| $l_a$ , $l_b$ | 34 mm, 300mm | – |
| $r$ | – | 33mm |
| Spring constant | – | 40 N/mm |

### B. Output torque

From Fig.1, the output torque of the traditional actuator can be expressed as:

$$T_o = \begin{cases} p_b A_b l_a \cos\varphi & \varphi_{l1} \to \varphi_{l2} \\ p_a A_a l_a \cos\varphi & \varphi_{l2} \to \varphi_{l1} \end{cases} \quad (24)$$

From Fig.3, the output torque of the new actuator is:

$$T_o = \begin{cases} p_c A_c r - k_s(y_{s0} + \varphi r) r & \varphi_{l1} \to \varphi_{l2} \\ k_s(y_{s0} + \varphi r) r - p_c A_c r & \varphi_{l2} \to \varphi_{l1} \end{cases} \quad (25)$$

If the pressure loss in the valve is neglected, we can get the maximum output torque for the two types of actuators with 20MPa supply pressure (Fig.7). It can be seen that the output torque of the new actuator has a linear relationship with rotary angle $\varphi$.

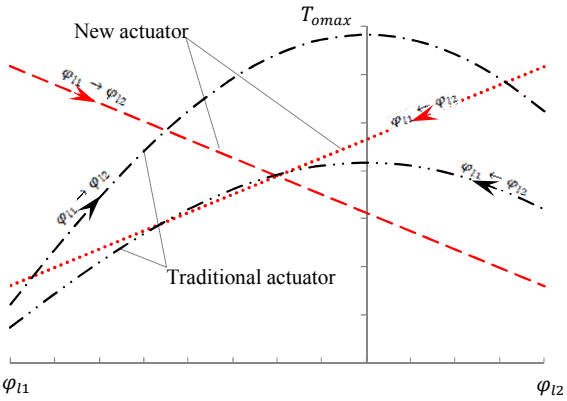

Fig.7 Maximum output torque

### C. Volumetric displacement

The actuator volumetric displacement $V_d$ is defined as the volume of fluid that flows in or out of the actuator per radian. Therefore, the volumetric displacement of the traditional actuator can be written as:

$$V_d = A_a \left|\frac{dl_c}{d\varphi}\right| = \frac{A_a l_a |l_a \sin\varphi - l_b \cos\varphi|}{\sqrt{l_b^2 + 2l_a^2 - 2l_a(l_b \sin\varphi + l_a \cos\varphi)}} \quad (26)$$

The volumetric displacement of the new actuator is:

$$V_d = A_c r \quad (27)$$

From (27) and (28), it can be seen that the volumetric displacement of the new actuator is a constant, while for a traditional actuator, this displacement highly depends on the rotary angle φ, This means, for a constant rotary speed motion, the exact amount of demanded flow can be supplied and hence less flow will pass through the relief valve. Therefore, higher efficiency is achieved.

### D. Other features

*1) No risk of buckling*

From Fig.5, it can be seen that the cylinder has no rotary motion and sustains only tensile stress. Therefore, there will be no risk of bending or breaking.

*2) Reduced pressure pulsations*

When the actuator reverses, the theoretical pressure in the cylinder chamber of the new actuator always equals $k_s(y_{s0} + y_s)/A_c$ if there is no load. If compared to the traditional actuator (Table I) the pressure jumps are smaller and it is possible for the new actuator to work smoothly when cylinder changes direction.

*3) Energy saving*

Compared to the traditional one, only one throttle orifice is used to control the flow, which reduces the energy loss of the flow through the valve. Furthermore, the spring can store energy and then release it during the next motion.

## VI. Conclusions and Future Work

In this work, a 3-way proportional valve controlled, spring assisted electro-hydraulic rotary actuator was presented and a mathematical model was developed. Comparison analyses were made between the new actuator and a traditional one. Several conclusions can be drawn as follows:

*1)* The output torque of the new actuator is linear with respect to the rotary angle for a constant input pressure.

*2)* The volumetric displacement of the new actuator is a constant.

*3)* There is no risk of buckling and little pressure pulsation in the new actuator.

*4)* High efficiency is achieved by reducing the throttle orifices.

Future work will include the following:

*1)* Prototyping of the 3-way valve-controlled spring assisted rotary actuator, as shown in Fig. 3.

*2)* Experimental and numerical studies to evaluate the performance in terms of output torque, volumetric displacement, dynamic response, efficiency and load capacity under different pressures and with different springs.

*3)* Optimization of the design based on experimental and numerical findings.

## References


[1] W.Backé, "Water or oil hydraulics in the future," *The Sixth Scandinavian International Conference on Fluid Power, SICFP'99*, pp. 51-65, Tampere, Finland, May 1999.

[2] Y.S. Yang, C. Semini, E. Guglielmino, N. G. Tsagarakis and D. G. Caldwell, " Water vs. oil hydraulic actuation for a robot leg," *IEEE Int. Conf. on Mechatronics and Automation* (*ICMA*), pp.1940-1946, Changchun, China, Aug 2009.

[3] D. G. Feldmann, "The use of ceramic materials for fluid power components," *80th Anniversary of Lithuanian University of Agriculture*, Kaunas, Lithuania, pp. 60-64, Oct. 2004.

[4] D. Van Bebber and H. Murrenhoff, "Improving the wear resistance of hydraulic machines using PVD-coating technology," *O+P Ölhydraulik und Pneumatik* Vol. 46, N. 11-12, pp.1-35, 2002.

[5] M. Linjama, M. Huova, P. Bostöm, A. Laamanen, L. Siivonen, L. Morel, M. Walden and M. Vilenius, "Design and Implementation of Energy Saving Digital Hydraulic Control System," *The Tenth Scandinavian Int. Conference on Fluid Power* (*SICFP'07*), Tampere, Finland, May 2007.

[6] A. B. Zoss, H. Kazerooni and A. Chu, "Biomechanical design of the Berkeley lower extremity exoskeleton [BLEEX]," *IEEE/ASME Transactions on Mechatronics*, Vol. 11, No. 2, pp. 128-138, 2006.

[7] Raytheon (2008) "The Exoskeleton: Advanced Robotics", Available: http://www.raytheon.com/newsroom/technology/rtn08_exoskeleton/

[8] S.H. Hyon, J.G. Hale, G. Cheng, "Full-Body Compliant Human–Humanoid Interaction: Balancing in the Presence of Unknown External Forces," *IEEE Trans. Robotics and Automation*, Vol. 23, N. 5, pp. 884-898, 2007.

[9] S. Hyon, S. Abe and T. Emura, "Development of a biologically inspired biped robot KenkenII," *Japan-France Congress on Mechatronics & 4th Asia Europe Congress on Mechatronics*, pp. 404-409, Sept.2003.

[10] M. Raibert, K. Blankespoor, G. Nelson, R. Playter and the Bigdog Team, "BigDog, the Rough-Terrain Quadruped Robot," *Proc. of the 17th IFAC World Congress*, pp. 10822-10825, Seoul, Korea, 2008.

[11] BostonDynamics, "PETMAN-BigDog gets a big brother," Available: http://www.bostondynamics.com/robot_petman.html

[12] C. Semini, N.G. Tsagarakis, B. Vanderborght, Y.S. Yang and D.G. Caldwell, "HyQ – hydraulically actuated quadruped robot: Hopping leg prototype," *IEEE/RAS Int. Conf. on Biomedical Robotics and Biomechatronics* (*Biorob*), pp.593-599, Scottsdale, Arizona, USA, 2008.

[13] E. Guglielmino, C. Semini, Y.S. Yang, D. G. Caldwell, H. Kogler and R. Scheidl, "Energy efficient fluid power in autonomous legged robotics," *ASME 2009 Dynamic Systems and Control Conference* (*DSCC2009*), Hollywood, LA, Oct. 2009.

[14] Y.S. Yang, C. Semini, N.G. Tsagarakis, E. Guglielmino and D.G. Caldwell, "Leg Mechanisms for Hydraulically Actuated Robots," *The 2009 IEEE/RSJ Int. Conf. on Intelligent Robots and Systems*, pp. 4699-4675, St. Louis, Oct. 2009.

[15] M. Focchi, E. Guglielmino, C. Semini, T. Boaventura, Y.S. Yang and D.G. Caldwell, "Control of a hydraulically-actuated quadruped robot leg," *IEEE Int. Conference on Robotics and Automation*, Anchorage, Alaska, 2010.

[16] C. Ridderstrom, J. Ingvast, F. Hardarson, M. Gudmundsson, M. Hellgren, J. Wikander and T. Wadden, "The basic design of the quadruped robot Warp1," *Int. Conf. on Climbing and Walking Robots* (*CLAWAR*), pp.87-94, Madrid, Spain, 2000.

[17] K. Ahn and S. Yokota, "Robust force control of a 6-link electro-hydraulic manipulator," *JSME International Journal Series C*, Vol. 46, No. 3, pp.1091-1099, 2003.

[18] N. D. Manring, *Hydraulic Control Systems*, John Wiley&Sons, New Jersey, 2005.